Eur Biophys J (2002) 31: 118–125
DOI 10.1007/s00249-001-0200-4

ARTICLE

C. Wilhelm · F. Gazeau · J.-C. Bacri

Magnetophoresis and ferromagnetic resonance of magnetically labeled cells

Received: 24 April 2001 / Revised: 7 November 2001 / Accepted: 7 November 2001 / Published online: 9 February 2002

Abstract We develop in this paper two methods, based on different physical concepts, to quantify the uptake of magnetic nanoparticles in biological cells. The first one, magnetophoresis, is based on the measurement of the velocity of magnetically labeled cells submitted to a magnetic field gradient. The second one quantitates the particles' electronic spin using an electron paramagnetic resonance experiment. We show a quantitative agreement between both methods for macrophagic cells. The uptake kinetics and uptake capacity are discussed for macrophagic cells and other cell lines.

Keywords Magnetic nanoparticles · Cell labeling · Magnetophoresis · Ferromagnetic resonance

Introduction

Magnetic particles from nanometer to micrometer size are involved in an increasing number of biological and medical applications. The magnetic labeling of cells can be be achieved through non-specific processes, but also specifically owing to the ability to target magnetic particles linked to a biological effector toward a cell receptor. The main developments of magnetic (immuno)labeling involve cell detection, cell sorting and organelles separation with the aid of a magnetic field gradient (Miltenyi et al. 1990; Radbruch et al. 1994; Moore et al. 1998; Kausch et al. 1999; Zborowski et al. 1999; Chemla et al. 2000; McCloskey et al. 2000; Raghavarao et al. 2000). Interest ranges from fundamental cellular biology to commercial assays. In the medical field, magnetic nanoparticles are known as contrast agents for magnetic resonance imaging (MRI), inducing an enhancement of proton relaxation. Their clinical use is mainly based on the rapid capture of magnetic nanoparticles by the cells of the reticuloendothelial system (as Kupfer cells of the liver) (Weissleder and Reimer 1993), but also in tumor cells (Moore et al. 1997, 2000). Besides, recent studies tend to associate signal amplification and targeting ability in order to image in vivo endogeneous or exogeneous (as in gene therapy) gene expression (Hogemann et al. 2000; Weissleder et al. 2000). Another challenge of the modern MRI technique is to track in vivo the distribution and motion of specific cells (Bulte et al. 1999) and eventually to recover magnetically the labeled cells from organs (Lewin et al. 2000). These recent trends are crucial in the development of cellular therapy for localization and retrieval of cell populations in vivo. However, the uptake of magnetic nanoparticles by the cells of interest is usually qualitatively demonstrated using electron microscopy or immunofluorescence assays (Schulze et al. 1995; Moore et al. 1997; Dodd et al. 1999), but is rarely quantified. Radiolabeling of the particles is sometimes associated with magnetic labeling to evaluate the particle load in cells (Schulze et al. 1995; Moore et al. 2000). In the field of MRI, NMR relaxometry measurements on cell samples or ex vivo organs are used to evaluate the particle concentration (Rety et al. 2000). The method is based on the proportionality between the proton relaxation rates (or inverse relaxation times) and the particle concentration in the sample. Nevertheless, the relaxivities of the particles (defined as the proportionality coefficient between the relaxation rate and the particle concentration) depend on their spatial distribution: they are drastically modified when particles are internalized in cells and concentrated in intracellular organelles compared to dispersed and isolated particles, for example in the blood pool (Oswald et al. 1997). It is therefore important to develop independent methods to

C. Wilhelm · F. Gazeau (✉) · J.-C. Bacri
Laboratoire des Milieux Désordonnés et Hétérogènes,
Centre National de la Recherche Scientifique,
Université Pierre et Marie Curie, Case 78,
4 Place Jussieu, 75252 Paris Cedex 05, France
E-mail: floga@ccr.jussieu.fr
Fax: +33-1-44-27-38-54

J.-C. Bacri
Université Paris 7, UFR de Physique,
2 Place Jussieu, Paris Cedex 05, France

quantify particle uptake in biological samples. With this objective, this paper presents two experimental techniques which are based on clearly different concepts. The first one, magnetophoresis, consists in determining the magnetically induced velocity of a magnetically labeled cell in a magnetic field gradient (Chalmers et al. 1999). The second one, ferromagnetic resonance (FMR), uses a classical EPR experiment to measure the iron content in a sample of about one million cells. Both assays are tested on a model cell system of mouse macrophages targeted with magnetic nanoparticles, using non-specific labeling. As an illustration, the loading capacity, the statistic uptake dispersion and the uptake kinetics are determined for the cell line. The paper is organized as follows. In the first section, materials and methods are described. We present in the next sections the results of both magnetophoresis and FMR quantification in the case of macrophagic cells phagocytizing magnetic nanoparticles and for other cell lines. The statistical analysis is thus discussed and both quantification assays are compared.

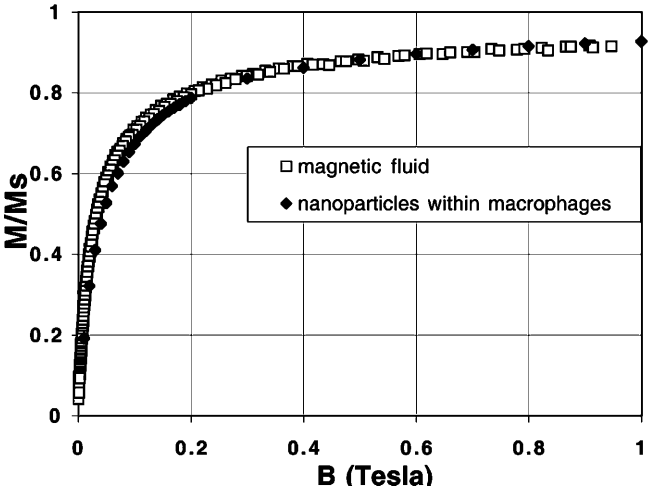

Fig. 1 SQUID measurements. Magnetization normalized by the magnetization saturation value as a function of the external magnetic field **B** for maghemite nanoparticles in water with [Fe] = 0.1 M (*squares*) and for nanoparticles internalized in macrophages (corresponding to [Fe] = 1 mM in the culture medium with 4 h incubation) (*diamonds*)

Materials and methods

Synthesis and characterization of the magnetic nanoparticles

The magnetic ionic nanoparticles used in the study are made of a magnetic ferric oxide, maghemite (γ-Fe_2O_3). They have been synthesized according to Massart's method (Massart 1981), by condensation of metallic salts in an alkaline medium. The particles are roughly spherical and magnetically monodomain. The magnetic anisotropy energy E_a is less than the thermal energy $k_B T$, so that the particles are superparamagnetic: their magnetic moments can rotate freely inside the grains. In order to obtain a biocompatible ferrofluid at pH 7, maghemite particles are coated with *meso*-2,3-dimercaptosuccinic acid (DMSA) (Halbreich et al. 1995; Fauconnier et al. 1997). They thus bear negative surface charges and repel each other through electrostatic interactions, ensuring the stability of the ferrofluid in aqueous solution. Particles in suspension are polydisperse and the size distribution is described by a log-normal law (Bacri et al. 1986):

$$P(d) = \frac{1}{\sqrt{2\pi}\sigma d}\exp\left[-\frac{1}{2\sigma^2}\left(\ln\frac{d}{d_0}\right)^2\right] \quad (1)$$

where d_0 is a characteristic diameter and σ the standard deviation. These two parameters are obtained by analyzing the magnetization curve, which is the superposition of classical Langevin laws for particles with diameter d (Bacri et al. 1987). The average diameter d_m can be estimated taking into account the polydispersity, that is:

$$d_m^3 = d_0^3 \exp\left(\frac{3^2\sigma^2}{2}\right) \quad (2)$$

Figure 1 presents the magnetization curve obtained for our magnetic fluid, allowing us to find a characteristic diameter $d_0 = 6.74$ nm, a standard deviation $\sigma = 0.42$ and an average diameter $d_m = 8.78$ nm, corresponding to 13700 iron atoms per particle.

Magnetic cell labeling

RAW 264.7 mouse macrophages were magnetically labeled. The cells were grown in RPMI 1640 medium (ATGC), supplemented with 10% heat-inactivated fetal calf serum (ATGC), 50 U/mL penicillin, 40 mg/mL streptomycin and 0.3 mg/mL L-glutamin. Macrophages (10^6 cells, 5 mL) were incubated for different times (15 min to 24 h) with magnetic particles (iron concentration from 0.01 mM to 10 mM) in a specific culture medium (LifeTechnologies, 11877-032), free of any potassium ions, in order to avoid particle floculation due to the screening of electrostatic interactions.

Electron micrographs (Fig. 2) of magnetically labeled macrophages show that particles are taken up by cells, following the endocytosis pathway. The particles first bind onto the plasma membrane through electrostatic interactions. They are subsequently internalized into early endosomes (100–200 nm diameter) that fuse later into larger organelles like late endosomes or lysosomes (0.5–1 μm diameter). These organelles contain 10^4–10^5 particles.

The magnetization of magnetically labeled cells (RAW macrophages, 4 h incubation at [Fe] = 1 mM) as a function of the external magnetic field is obtained using a superconducting quantum interference device (SQUID) and is illustrated in Fig. 1 in comparison with the magnetization of the magnetic fluid used for the cell labeling. Magnetically labeled cells present a magnetization slightly lower than the ferrofluid in the low-field range $B < 400$ mT. Owing to their confinement in roughly spherical endosomes, particles within the cells experience a demagnetizing field that reduces their global magnetization.

Assays to quantify particle cellular uptake

Cell magnetophoresis

Principle

The analogy of cell magnetophoresis with the well-known cell electrophoresis must be considered with caution: contrary to electrophoresis, where charge movement is driven by a uniform electric field, a magnetic moment can experience a magnetic force only in the presence of a magnetic field gradient $\vec{\nabla}B$. Magnetically labeled cells bearing a global magnetic moment $\vec{M}$ are thus attracted in the region of the maximum magnetic field. As the carrier medium for the cells is non-magnetic, the magnetic force that puts magnetically labeled cells in suspension into motion is:

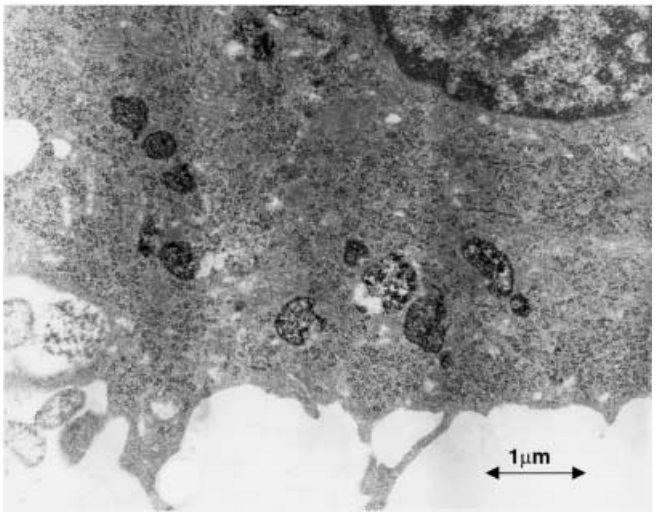

Fig. 2 Electron micrograph of a macrophagic cell having internalized magnetic nanoparticles for 4 h with an iron concentration in the liquid medium of 1 mM. Nanoparticles are concentrated within intracellular organelles

$$\vec{F}_{\mathrm{m}} = \left(\vec{M}.\vec{\nabla}\right)\vec{B} \tag{3}$$

where $\vec{B}$ is the magnetic field experienced by the cell. The total magnetic moment of the cell, $\vec{M}$, is simply the product of the effective magnetization, $\vec{m}_{\mathrm{eff}}$, of one particle in the field $\vec{B}$ by the total number N of particles within the cell: $\vec{M} = N\vec{m}_{\mathrm{eff}}$. Cells moving in a liquid medium are submitted to a hydrodynamic drag force, $\vec{F}_{\mathrm{d}}$. At low Reynolds number, assuming a perfect sphere for the cell, $\vec{F}_{\mathrm{d}}$ is given by Stokes law:

$$\vec{F}_{\mathrm{d}} = -3\pi\eta D\vec{v} \tag{4}$$

where D is the cell diameter, η is the viscosity of the carrier liquid and $\vec{v}$ is the cell velocity. In a permanent regime, $\vec{F}_{\mathrm{d}}$ counterbalances the magnetic force so that the velocity measurement of each cell leads to the cell magnetization and particle load N.

Set-up

The apparatus is mainly composed of a permanent circular magnet. Cells containing particles migrate toward the magnet, while the motion is observed with a microscope objective, 6 mm away from the center of the magnet (Fig. 3). A digital camera is used to record cell movement and a graphic card allows video analysis. The magnetic field was measured at each point using a gaussmeter and a Hall effect probe. A micrometric displacement was used to control the position of the probe in the magnetic field. We plot in Fig. 4 the magnetic field vectors and the magnetic field lines in a plane (x, z) perpendicular to one magnet diameter, using measured values of the magnetic field components B_x and B_z, and assuming spherical symmetry. Consequently, in the observation window ($z = 6$ mm, $x = 0 \pm 0.2$ mm), the magnetic field as well as the magnetic field gradient are uniform:

$$\vec{B} = B\vec{e}_z,\ B = 174\ \mathrm{mT} \quad \vec{\nabla}B = \tfrac{\mathrm{d}B}{\mathrm{d}z}\vec{e}_z,\ \tfrac{\mathrm{d}B}{\mathrm{d}z} = 18.5\ \mathrm{mT/mm} \tag{5}$$

For a 174 mT magnetic field, the cell magnetization corresponds to 75% of its saturation value M_s, as seen in Fig. 1. Thus the effective magnetic moment, m_{eff}, of each particle in a cell migrating in the observation window is:

$$m_{\mathrm{eff}} = (0.75M_s)\frac{\pi}{6}d_{\mathrm{m}}^3 \tag{6}$$

where $M_s = 3.1\times10^5$ A/m^2 is the volumic saturation magnetization for maghemite particles. We can thus derive the magnetic force acting on a cell of magnetic moment $M = Nm_{\mathrm{eff}}$:

$$\vec{F}_{\mathrm{m}} = Nm_{\mathrm{eff}}\frac{\mathrm{d}B}{\mathrm{d}z}\vec{e}_z \tag{7}$$

We observe experimentally the permanent regime of constant cell velocity, where the magnetic force $\vec{F}_{\mathrm{m}}$ balances the drag force $\vec{F}_{\mathrm{d}}$. The determination of one cell velocity v leads to the number N of particles loaded by the cell, following the relation:

$$N = \frac{3\pi\eta D}{m_{\mathrm{eff}}\frac{\mathrm{d}B}{\mathrm{d}z}}v \tag{8}$$

Experimental

After incubation with particles, cells were washed three times, scraped in 4 mL RPMI and centrifuged at 1100 rpm for 10 min. Macrophages were then dispersed in RPMI at a concentration of 10^4 cells/mL and 0.4 mL of the solution was introduced into a 1-mm thick Hellma chamber, which was previously treated with dimethyldichlorosilane to prevent cells from adhering to the glass. For each incubation time or iron concentration in the culture medium, the velocity of 100 cells was determined using the video records of the moving cells. Figure 5 shows a typical distribution of cell velocities. One can directly obtain from Eq. (8) the distributions of the number of particles loaded by cells. Figure 6 is an illustration of such histograms for two different incubation times and two different iron concentrations in the culture medium.

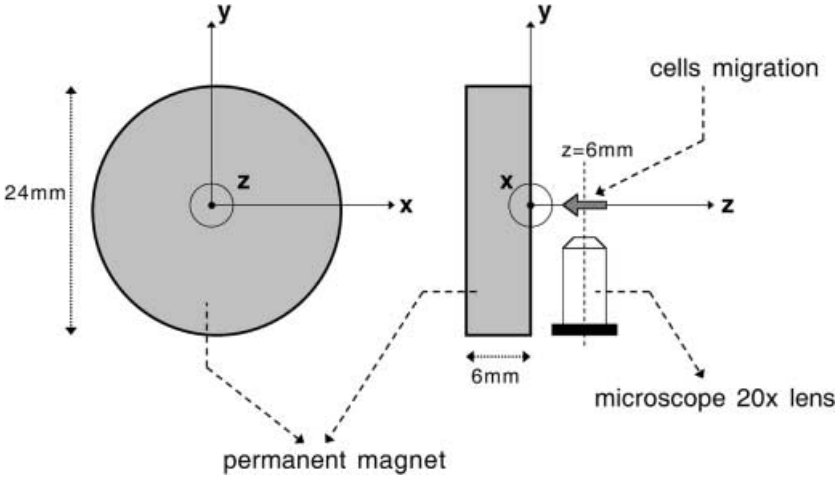

Fig. 3 Experimental device for magnetophoresis measurements. The Hellma chamber containing magnetically labeled cells in suspension is placed perpendicularly to a circular permanent magnet. The cell movements are observed 6 mm apart from the magnet through a 20× microscope lens

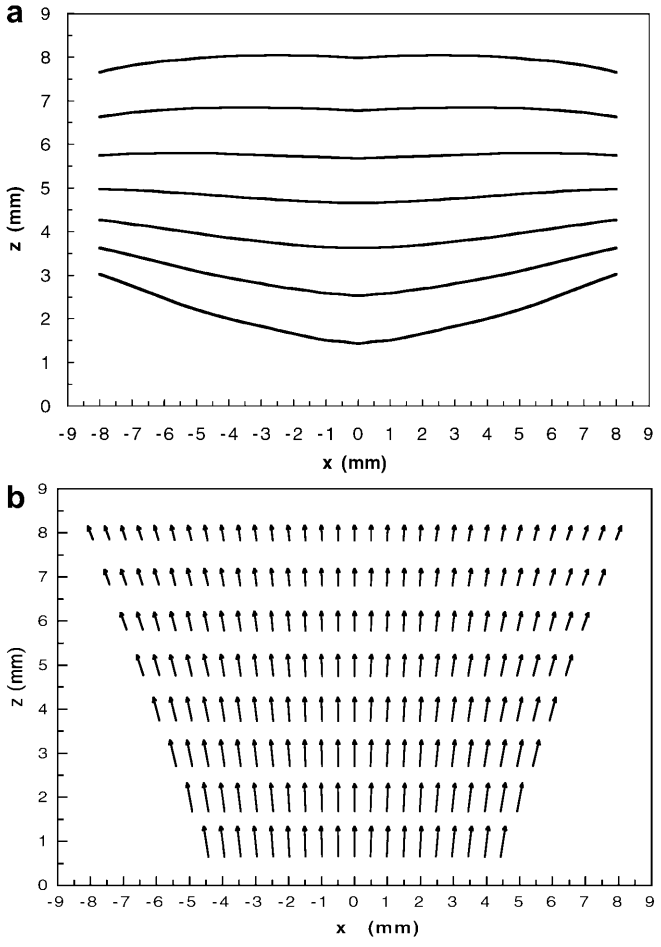

Fig. 4 **a** Magnetic field line representation of the field created by the permanent circular magnet. **b** Vector plot of the magnetic field

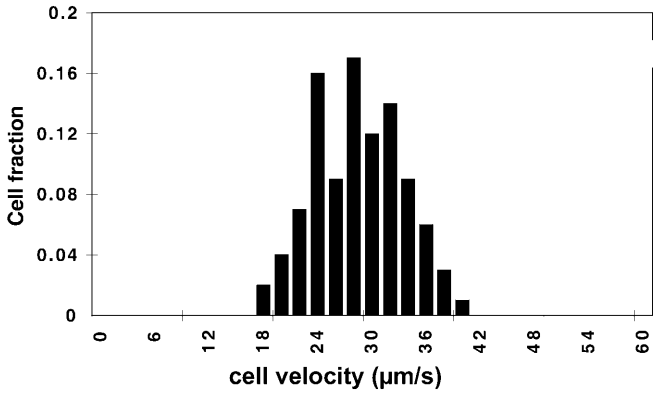

Fig. 5 Distribution of the velocity of magnetically labeled macrophages obtained by magnetophoresis (3 h incubation time, [Fe] = 0.75 mM)

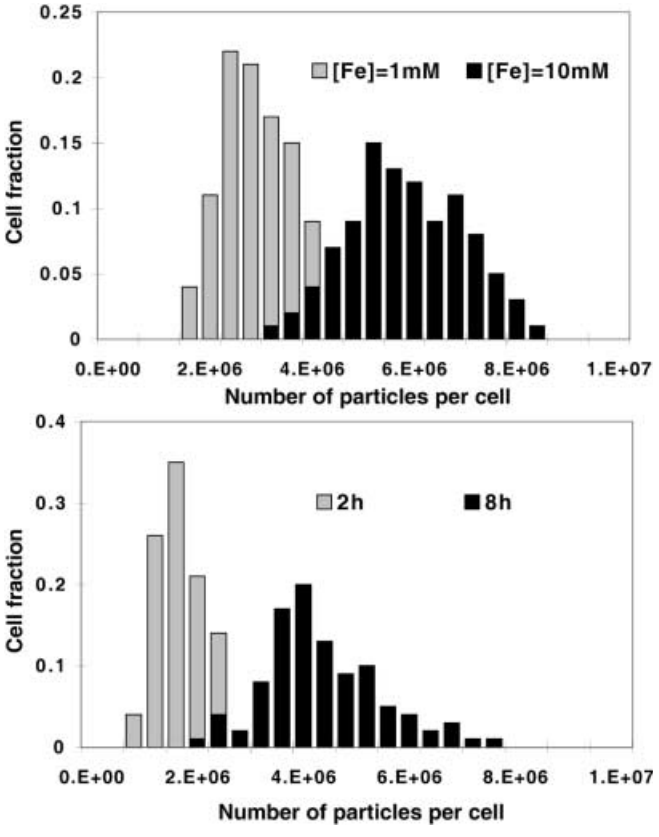

Fig. 6 *Top* Distributions of the number of particles internalized by cells corresponding to 4 h incubation and respectively 1 mM and 10 mM iron concentration. *Bottom* Distributions of the number of particles internalized by cells for [Fe] = 0.75 mM and respectively 2 h and 8 h incubation

Ferromagnetic resonance

Principle

FMR consists in classical EPR allowing quantification of electronic spins in a sample (Chang and Kahn 1978). However, instead of detecting the resonance of individual electronic spins, we consider here macrospins resulting from the exchange interaction in the ferrimagnetic lattice constituting the particle core (Gazeau et al. 1998, 1999). FMR can be used to measure the amount of macrospins of known spectrum in a sample. The hyperfrequency field which drives the resonance has a fixed frequency of 9.2 GHz. The experimental set-up provides a recording of the derivative $\frac{dP}{dH}$ of the microwave absorption curve with respect to the constant magnetic field H (see Fig. 7). By measuring the absorption curve of aqueous ferrofluid samples at different iron concentrations, we have demonstrated that the area under the EPR absorption curve, $\int P(H)\mathrm{d}H$, linearly depends upon the number of macrospins in the sample or equivalent moles of particulate iron. Using this calibration, a unit area, which is to the lowest quantitable adsorption signal, corresponds to 4.5×10^{-11} moles of iron (or equivalently, 2×10^{9} particles in the sample under consideration).

Experimental

After incubation with the particles, the cells were washed three times, scraped in 4 mL RPMI and centrifuged at 1100 rpm for 10 min. The cell pellet was resuspended in 50 μL PBS and 5 μL were introduced into a glass disposable micropipette, which was placed in a quartz tube suitable for EPR experiments. The number of cells per microliter being known, after two integrations of the EPR signal the average number of particles per cell is obtained. As an illustration, Fig. 7 shows the EPR spectra for samples corresponding to increasing incubation times with the same iron concentration in the culture medium.

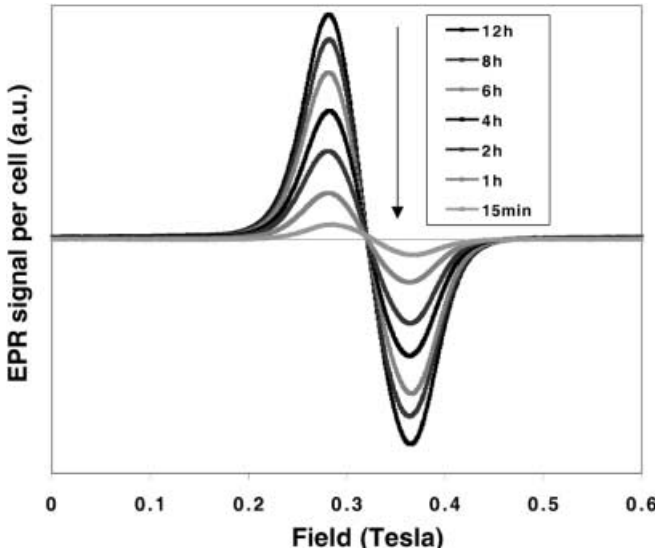

Fig. 7 EPR absorption spectra normalized to one cell for cells having internalized particles during different incubation times, with the same iron concentration in the liquid medium ([Fe] = 0.5 mM)

Results

Magnetophoresis and FMR are performed on macrophages, on the one hand for a fixed iron concentration in the liquid medium of [Fe] = 0.75 mM and incubation times varying from 15 min to 24 h, and, on the other hand, for two fixed incubation times (1 h and 4 h) and iron concentrations ranging from 0.1 mM to 10 mM. For each experiment, the amount of particles internalized in cells during the incubation is negligible compared to the amount of particles in the extracellular medium, allowing us to consider an infinite reservoir of particles. As shown in Fig. 8 for macrophages, we note the excellent agreement between magnetophoresis and FMR measurements. As illustrated in Fig. 8 (top), the particle uptake tends exponentially to a saturation value as the incubation time is increased:

$$N(t) = N_{\max}([Fe])\left[1 - \exp\left(-\frac{t}{\tau([Fe])}\right)\right] \quad (9)$$

The rate $\frac{dN}{dt}$ of particle internalization therefore decreases as an exponential as a function of time. The saturation of the number of internalized particles is interpreted as a loading capacity, $N_{\max}([Fe])$, depending on the particle concentration in the liquid medium. The particle uptake depends upon the extracellular iron concentration (see Fig. 8 bottom):

$$N([Fe]) = N_{\max}(t)\left[1 - \exp\left(-\frac{[Fe]}{[Fe]_0(t)}\right)\right] \quad (10)$$

An internalization rate $\frac{dN}{d[Fe]}$, decreasing exponentially as a function of [Fe], can be defined as well as a loading

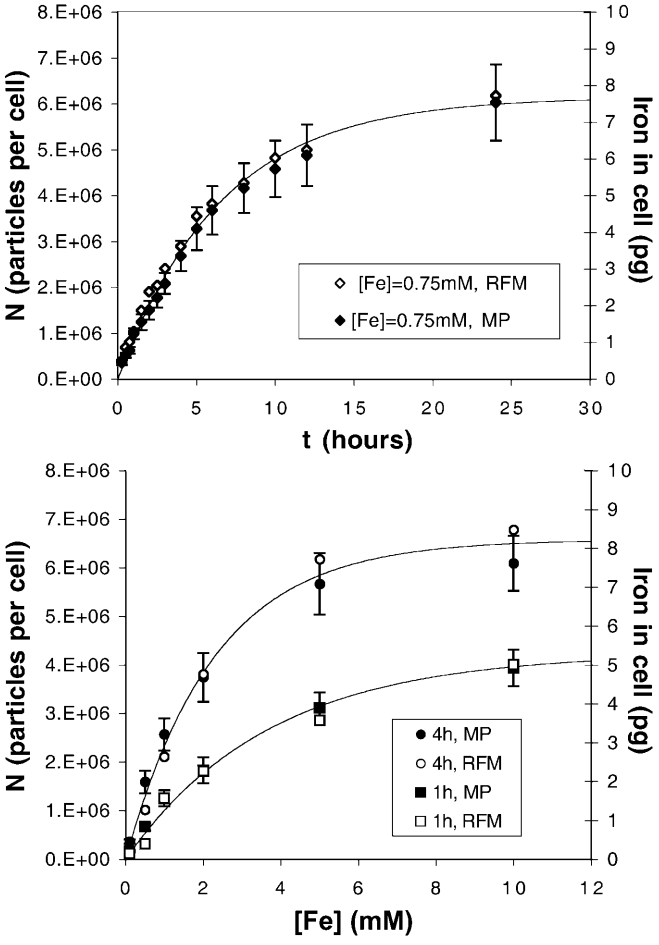

Fig. 8 Magnetophoresis (MP) and ferromagnetic resonance (FMR) quantitations of magnetic nanoparticle uptake in RAW mouse macrophages. *Top* Evolution of the number of particles internalized per cell for different incubation times with the same iron concentration in the liquid medium ([Fe] = 0.75 mM). *Bottom* Dependence of particle internalization with the iron concentration in the medium for two different incubation times ($t = 1$ h and 4 h). Magnetophoresis measurements are shown with the statistical deviation ΔN obtained from the distribution of the particle uptake. For each condition, the exponential fit is drawn as a *curved line*

capacity $N_{\max}(t)$. The parameters $\frac{dN}{dt}([Fe], t = 0)$, $\frac{dN}{d[Fe]}([Fe] = 0, t)$ and $N_{\max}([Fe], t)$ are the mean characteristics of a cell line. They are given in Table 1 for macrophagic mouse cells. Though the FMR measurement only provides the average number of internalized particles in a cell sample, the histograms obtained from magnetophoresis experiments lead to the relative dispersion $\frac{\Delta N}{N}$ of the number of internalized particles, reflecting the variation of uptake ability from cell to cell. The relative dispersion $\frac{\Delta N}{N}$ is represented in Fig. 9 as a function of incubation time and as a function of extracellular iron concentration. It is approximatively constant (between 0.20 and 0.28) with respect to both parameters. Thus, there exist macrophages with low particle uptake capacity as well as cells with high particle uptake capacity. However, it is remarkable that for macrophages the relative dispersion of particle uptake,

$\frac{\Delta N}{N}$, depends neither upon the extracellular iron concentration nor upon the time of internalization. It means that, whatever the external conditions, the behavior of the whole cell population is self similar and depends only upon the cell type in the particulate culture conditions.

Magnetophoresis experiments were performed for other cell lines. The results are presented in Table 2 for human dendritic cells, T-lymphocytes and pulmonary epithelium cells (A549). The different particle uptakes are characteristic of the cell lines. For dentritic cells and T-lymphocytes, particle uptake is quantified for different iron concentrations and incubation times. Histograms of cell velocity for both cell lines and for one specific incubation condition are presented in Fig. 10 and clearly illustrate the efficiency of cell sorting under a magnetic field gradient.

Table 1 Parameters of the particle uptake in macrophages deduced from the exponential fits using Eqs. (9) and (10)

Time dependence
$N_{max}([Fe] = 0.75\ mM) = (6.15 \pm 0.11) \times 10^6$ particles
$\tau([Fe] = 0.75\ mM) = (6.57 \pm 0.12)$ h
Iron concentration dependence
$N_{max}(t = 1\ h) = (4.25 \pm 0.16) \times 10^6$ particles
$[Fe]_0(t = 1\ h) = 3.66 \pm 0.16$ mM
$N_{max}(t = 4\ h) = (6.58 \pm 0.19) \times 10^6$ particles
$[Fe]_0(t = 4\ h) = 2.28 \pm 0.18$ mM

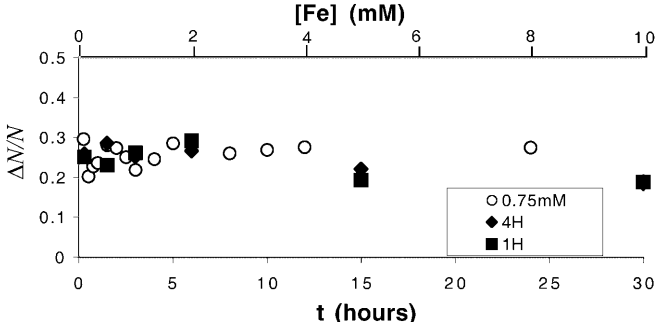

Fig. 9 Evolution of the relative dispersion $\frac{\Delta N}{N}$ with respect to the incubation time t (for [Fe] = 0.75 mM) and with respect to the iron concentration [Fe] in the liquid medium (for $t = 1$ h and 4 h)

Discussion and conclusion

As demonstrated in Fig. 8, the two assays presented here, although they are based on different physical concepts, lead to the same quantitative results. The principles and technical limitations are different for both methods. Magnetophoresis is based on a hydrodynamic measurement. Measurements in a permanent regime are required for the balance force equation [see Eqs. (3, 4)] to be valid: with our set-up, the permanent regime can be achieved since the magnetic field gradient (as well as the cell magnetization) is uniform in the observation window. The main limitation consists of adjacent hydrodynamic flows that eventually perturb the magnetically induced cell motion. It can occur, for example, when a cell aggregate rapidly migrates. It is therefore crucial to measure the cell velocity for highly diluted and isolated cells to avoid hydrodynamic and magnetic interactions. The second

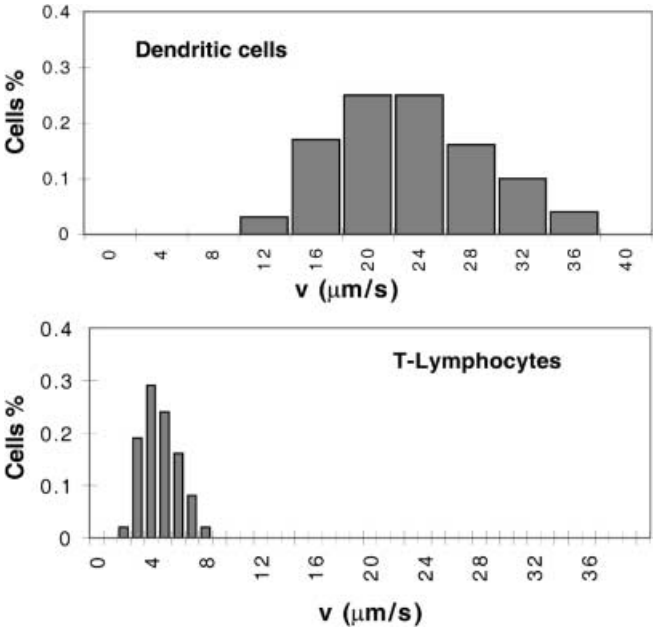

Fig. 10 Histograms of the particle uptake in dendritic cells or T lymphocytes for 1 h incubation with [Fe] = 0.3 mM in the culture medium

Table 2 Particle uptake in different human cell lines: dentritic cells, T-lymphocytes and epithelium cells. The number of particles internalized per cell is given together with its deviation obtained from the magnetophoresis distribution

Dendritic cells			
	0.15 mM	0.3 mM	0.6 mM
1 h	$9.28 \times 10^5 \pm 2.40 \times 10^5$	$1.56 \times 10^6 \pm 3.8 \times 10^5$	$1.90 \times 10^6 \pm 7.3 \times 10^5$
2 h	$9.92 \times 10^5 \pm 2.42 \times 10^5$	$2.05 \times 10^6 \pm 5.1 \times 10^5$	$2.84 \times 10^6 \pm 9.4 \times 10^5$
4 h	$1.13 \times 10^6 \pm 2.8 \times 10^5$	$2.98 \times 10^6 \pm 9.5 \times 10^5$	–
T-lymphocytes			
	0.15 mM	0.3 mM	0.6 mM
1 h	–	$1.87 \times 10^5 \pm 6.67 \times 10^4$	$4.85 \times 10^5 \pm 2.01 \times 10^5$
2 h	$9.52 \times 10^5 \pm 3.41 \times 10^5$	$3.80 \times 10^5 \pm 1.51 \times 10^5$	$6.92 \times 10^5 \pm 2.66 \times 10^5$
4 h	$1.79 \times 10^5 \pm 6.5 \times 10^5$	$7.76 \times 10^5 \pm 2.82 \times 10^5$	$1.36 \times 10^6 \pm 4.6 \times 10^5$
Epithelium cells			
	0.5 mM	5 mM	
3 h	$3.23 \times 10^6 \pm 5.8 \times 10^5$	$1.22 \times 10^6 \pm 2.8 \times 10^5$	

limitation in magnetophoresis assay is due to cell sedimentation in the Hellma chamber. Indeed, a cell containing 10^4 particles should have a velocity of 0.1 μm/s, becoming undetectable simply because of cell sedimentation, corresponding to a velocity around 2 μm/s: cells fall to the wall of the Hellma chamber during the time of the experiment and tend to adhere. In practice, owing to these experimental limitations, we are not able to measure cell velocities lower than 1 μm/s, corresponding to 0.1 pg of particulate iron loaded by the cell. FMR allows us to quantify electronic spins contained in a low volume sample. In principle, as low as 10^{11} spins can be detected with this resonance technique. In practice, for ferrimagnetic particles a unit area can be measured with good accuracy, corresponding to about 2×10^9 particles per sample or to approximatively 2×10^3 pg of particulate iron. Thus the lowest load which can be detected in magnetically labeled cells depends on the number of cells in the sample. For material containing a high degree of water, such as cell samples, low volumes (1–100 μL) are required in order to limit the increase of dielectric constant so that the RF cavity is accordable. In practice, a concentrated pellet containing one million cells in a 5 μL capillary tube can be sampled, allowing us to measure as few as 2×10^3 particles per cell. As a conclusion, we obtain noticeable agreement between FMR and magnetophoresis methods to quantify particle uptake in biological cells. In particular, our experiments confirm the assumption of proportionality between the magnetic force (or cell velocity) and the number of particles taken up. Moreover, the numerical factors as deduced from the magnetization curve (for magnetophoresis) and from the calibration (for FMR) using ferrofluid samples with different concentrations happen to coincide and only depend upon the particle type and size. The FMR quantitation permits us to validate the magnetophoresis assay, which reveals itself to be an accurate and simple method to quantify the particle uptake distribution for a cell culture, to obtain statistical data on the cell population and to evaluate the separation process for several cell lines in suspension or to slice populations with different particle loads in the same cell line. Conversely, the FMR assay can be extensively used for cells on different substrates and also for tissue samples of ex vivo organs, thus constituting a choice method for biodistribution analysis.

Acknowledgements We thank J. Roger and J.N. Pons (L2IC, University Paris 6) for providing the magnetic nanoparticles. We also thank B. de Crossa (Laboratoire d'embryologie, University Paris 5) for preparing the electron microscopy samples. We are grateful to F. Gendron (LMDH, University Paris 6) for giving us the opportunity to work on the EPR set-up and to L. Legrand (GPS, University Paris 6 and 7) for the SQUID measurements.

References

Bacri J-C, Perzynski R, Salin D, Cabuil V, Massart R (1986) Magnetic colloidal properties of ionic ferrofluids. J Magn Magn Mater 62:36–46

Bacri J-C, Cabuil V, Massart R, Perzynski R, Salin D, Cabuil V (1987) Ionic ferrofluid: optical properties. J Magn Magn Mater 65:285–288

Bulte JW, Zhang S, Gelderen P van, Herynek V, Jordan EK, Duncan ID, Frank JA (1999) Neurotransplantation of magnetically labeled oligodendrocyte progenitors: magnetic resonance tracking of cell migration and myelination. Proc Natl Acad Sci USA 96:15256–15261

Chalmers JJ, Haam S, Zhao Y, McCloskey K, Moore L, Zborowski M, Williams PS (1999) Quantification of cellular properties from external fields and resulting induced velocity: magnetic susceptibility. Biotechnol Bioeng 64:519–526

Chang T, Kahn AH (1978) Electron paramagnetic resonance intensity standard: description and use. Publ Natl Bur Stand August:1–49

Chemla YR, Grossman HL, Poon Y, McDermott R, Stevens R, Alper Clarke J (2000) Ultrasensitive magnetic biosensorfor homogeneous immunoassay. Proc Natl Acad Sci USA 97:14268–14272

Dodd SJ, Williams M, Suhan JP, Williams DS, Koretsky AP, Ho C (1999) Detection of single mammalian cells by high-resolution magnetic resonance imaging. Biophys J 76:103–109

Fauconnier N, Pons JN, Roger J, Bee A (1997) Thiolation of maghemite nanoparticles by dimercaptosuccinic acid. J Colloid Interface Sci 194:427–433

Gazeau F, Bacri J-C, Gendron F, Perzynski R, Raikher YuL, Stepanov VI, Dubois E (1998) Magnetic resonance of ferrite nanoparticles: evidence of surface effects J Magn Magn Mater 186:175–187

Gazeau F, Shilov V, Bacri J-C, Dubois E, Gendron F, Perzynski R, Raikher YuL, Stepanov VI (1999) Magnetic resonance of ferrite nanoparticles: evidence of thermofluctuational effects J Magn Magn Mater 202:535–546

Halbreich A, Sabolovic D, Sestier C, Geldwerth D, Pons JN, Roger J (1995) Nanoparticules magnetiques couplees a l''annexine et leur utilisation. Fr Pat 9507865 (PCT/FR96/00964, no. de publication 2736197). INPI, Paris

Hogemann D, Josephson L, Weissleder R, Basilion JP (2000) Improvement of MRI probes to allow efficient detection of gene expression. Bioconjug Chem 11:941–946

Kausch AP, Owen TP Jr, Narayanswami S, Bruce BD (1999) Organelle isolation by magnetic immunoabsorption. Biotechniques 26:336–343

Lewin M, Carlesso N, Tung CH, Tang XW, Cory D, Scadden DT, Weissleder R (2000) Tat peptide-derivatized magnetic nanoparticles allow in vivo tracking and recovery of progenitor cells. Nat Biotechnol 18:410–414

Massart R (1981) Preparation of aqueous magnetic liquids in alkaline and acidic media. IEEE Trans Magn 17:1247–1248

McCloskey KE, Chalmers JJ, Zborowski M (2000) Magnetophoretic mobilities correlate to antibody binding capacities. Cytometry 40:307–315

Miltenyi S, Muller W, Weichel W, Radbruch A (1990) High gradient magnetic cell separation. Cytometry 11:231–238

Moore A, Weissleder R, Bogdanov A (1997) Uptake of dextran-coated monocrystalline iron oxides in tumor cells and macrophages. J Magn Reson Imaging 7:1140–1145

Moore A, Marecos E, Bogdanov A Jr, Weissleder R (2000) Tumoral distribution of long-circulating dextran-coated iron oxide nanoparticles in a rodent model. Radiology 214:568–574

Moore LR, Zborowski M, Sun L, Chalmers JJ (1998) Lymphocyte fractionation using immunomagnetic colloid and dipole magnet flow cell sorter. J Biochem Biophys Methods 37:11–33

Oswald P, Clement O, Chambon C, Schouman-Claeys E, Frifa G (1997) Liver positive enhancement after injection of superparamagnetic nanoparticles: respective role of circulating and uptaken particles. Magn Reson Imaging 15:1025–1031

Radbruch A, Mechtold B, Thiel A, Miltenyi S, Pfluger E (1994) High gradient magnetic sorting. Methods Cell Biol 42:387–403

Raghavarao KS, Dueser M, Todd P (2000) Multistage magnetic and electrophoretic extraction of cells, particles and macromolecules. Adv Biochem Eng Biotechnol 68:139–190

Rety F, Clement O, Siauve N, Cuenod CA, Carnot F, Sich M, Buisine A, Frija G (2000) MR lymphography using iron oxide nanoparticles in rats: pharmacokinetics in the lymphatic system after intravenous injection J Magn Reson Imaging 12:734–749

Schulze E, Ferrucci JJ, Poss K, LaPointe L, Bogdanova A, Weissleder R (1995) Cellular uptake and trafficking of a prototypical magnetic iron oxide label in vitro. Invest Radiol 30:604–610

Weissleder R, Reimer P (1993) Superparamagnetic iron oxides for MRI. Eur J Radiol 3:198–212

Weissleder R, Moore A, Mahmood U, Bhorade R, Benveniste H, Chiocca EA, Basilion JP (2000) In vivo magnetic resonance imaging of transgene expression. Nat Med 6:351–355

Zborowski M, Sun L, Moore LR, Chalmers JJ (1999) Rapid cell isolation by magnetic flow sorting for applications in tissue engineering. ASAIO J 45:127–130